Journal of Coastal Research	33	4	747–763	Coconut Creek, Florida	July 2017

Estuarine Mangrove Squeeze in the Mekong Delta, Vietnam

Son Hong Truong[†‡], Qinghua Ye[†§], and Marcel J.F. Stive[†]*

[†]Faculty of Civil Engineering and Geosciences
Delft University of Technology
Delft 2628 CN, The Netherlands

[‡]Faculty of Civil Engineering
Water Resources University
Hanoi, Vietnam

[§]Deltares
Delft 2629 HV, The Netherlands

www.cerf-jcr.org

www.JCRonline.org

ABSTRACT

Truong, S.H.; Ye, Q., and Stive, M.J.F., 2017. Estuarine mangrove squeeze in the Mekong Delta, Vietnam. *Journal of Coastal Research,* 33(4), 747–763. Coconut Creek (Florida), ISSN 0749-0208.

Although the protective role of mangroves for coasts has been increasingly recognized, that of estuarine mangroves is less well acknowledged. The complex root, stem, and canopy system of healthy estuarine mangroves efficiently reduces the impact of a strong, along-bank flow during high tides and high river discharge, protecting the riverbank from eroding. If a sediment source is available, a healthy mangrove forest also offers a higher potential for sedimentation to compensate for sea-level rise. Unfortunately, along the Mekong, Vietnam, estuaries, mangroves have been rapidly destroyed. In many regions, estuarine mangroves have degraded into narrow strips of <50 m. Riverbanks at those locations are eroding at a rate of 2–4 m y^{-1}. The main reason for this "estuarine mangrove squeeze" phenomenon is due to the increasing demand to create more space for local fish farming. Hence, *squeeze* is used in a broader sense than in the context of sea-level rise impact alone. The hypothesis is that there is a critical minimum width for an estuarine mangrove forest strip to maintain its ability to survive. The analysis of available data, both from literature and from satellite observations, supports the hypothesis: An average critical width for Mekong estuaries was found to be approximately 80 m. To obtain insight into the efficiency of a mangrove forest in reducing the impacts of alongshore flow, the state-of-the-art Delft3D model was applied to the data. The model showed that the penetration-length scale of the shear layer into a mangrove forest requires a certain minimum space to develop fully. It is hypothesized that the minimum width of a mangrove forest, which equals this maximum penetration-length scale, has a crucial role for the health of a mangrove system.

ADDITIONAL INDEX WORDS: *Riverbank erosion, fish farm, critical width, flow penetration.*

INTRODUCTION

The Mekong Deltaic River System in Vietnam, located in the southern part of the country, covers an area of 39,000 km^2. Near its outlet to the sea, but still in Cambodia, as part of the Mekong Delta plain, the Mekong River divides into two branches, the Mekong (Tien River) and the Bassac (Hau River). Before reaching the sea, the Tien River and the Hau River then divide again into nine branches, which flow into nine estuaries, of which, presently, only eight estuaries are left (Tri, 2012). These estuaries, with complex multichannel systems, reach the South China Sea at the eastern zone of the Mekong Delta coast from the Tien Giang province to the Soc Trang province. This estuarine environment was the study area (Figure 1).

The Mekong Delta region in Vietnam is a tropical monsoon region. The dry season is from November to April, and the wet season is from May to October. The total mean river discharge of the Mekong is about 15,000 $m^3 s^{-1}$ (Lu and Siew, 2006). The mean high discharge during the flood season is 25,000 $m^3 s^{-1}$, and the mean low discharge during the dry season is 5000 $m^3 s^{-1}$.

According to the report of the Road and Hydraulic Engineering Institute (DWW, 2004), the local population suggests that erosion problems have increased since the 1990s in the Mekong Delta, in general, and in the Mekong Estuarine System (MES), in particular. There are several possible explanations for the accelerated erosion problems: (1) increasing sea level (Alongi, 2008; Webb *et al.*, 2013), (2) increasingly reduced sediment influx because of the construction of dams upstream of the Mekong River and sand mining, (3) increasing human-induced subsidence and groundwater extraction (International Union for Conservation of Nature, 2011), (4) the clearance of mangrove forests in the 1990s (Gebhardt, Dao Nguyen, and Kuenzer, 2012), and (5) the "squeeze" of the coastal mangrove forests. These are the reasons given for accelerated erosion along the coastal region (Phan, van Thiel de Vries, and Stive, 2014), and estuarine mangroves probably suffer from the same causes. Together with the accelerated erosion, in many regions along the MES, mangroves have degraded into a narrow strip of <50 m. Riverbanks at those locations are usually observed to be suffering from erosion at a rate of 2–4 m y^{-1} (Figure 2).

During floods, the Mekong Delta carries a large sediment load. The total annual sediment discharge of the entire Mekong Delta River was estimated to be about 160 million ton y^{-1} in 1995 (Milliman *et al.*, 1995) and about 110 million ton y^{-1} in 2011 (Milliman and Farnsworth, 2011). However, the amount of sediment that finally reaches the South China Sea is less than the total sediment carried by the Mekong River (Kummu and Varis, 2007). Only about 60% of the total sediment load enters the lower Mekong regions (Manh *et al.*, 2014). This means that the annual amount of sediment entering the lower Mekong basin is about 96 and 66 million ton y^{-1} in 1995 and 2011, respectively. An alternative estimation is based on the

DOI: 10.2112/JCOASTRES-D-16-00087.1 received 16 May 2016; accepted in revision 9 November 2016; corrected proofs received 5 January 2017; published pre-print online 20 March 2017.
*Corresponding author: m.j.f.stive@tudelft.nl

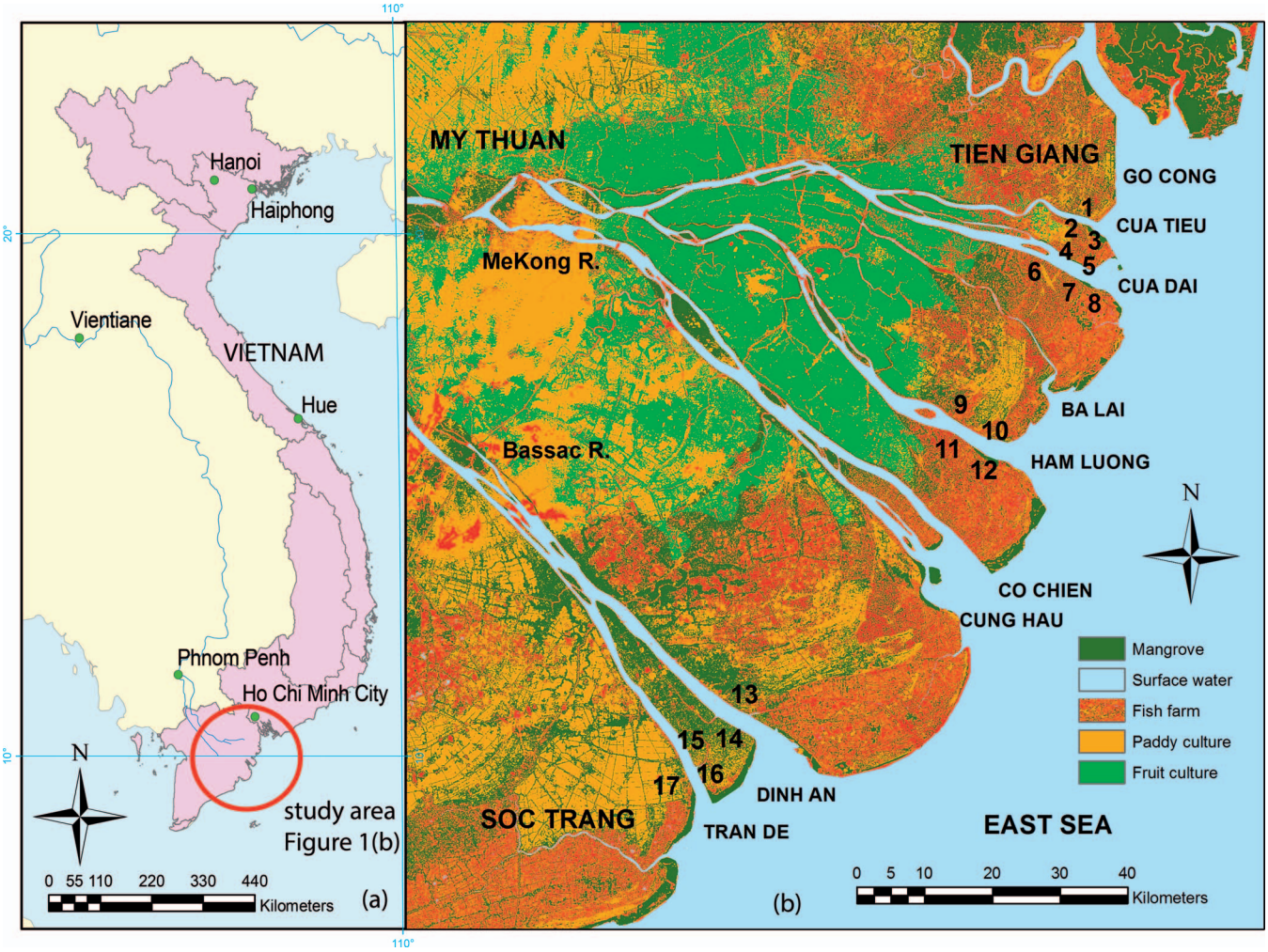

Figure 1. (a) Location of the study area in SE Asia. (b) Map of the Mekong Estuarine System captured from a Landsat image showing the major distribution of mangroves, fish farms, and fruit and paddy cultures in 2015. Mangroves were primarily located along the riverbanks and the coastal fringes. The locations numbered 1–17 were chosen for analysis of the evolutionary trend of the estuarine riverbank in relation to the mangrove forest width (specified in Table 1).

average suspended sediment concentrations (SSC), reaching approximately 50 mg L^{-1} and 80 mg L^{-1} from 1993 to 2000 at Can Tho and My Thuan stations, respectively (Lu and Siew, 2006). From the total mean discharge and the SSC, the total annual suspended sediment in the Mekong River can be estimated at about 38 million tons. For a sand-bed river, the bed-load fraction may be assumed to be around 30–50% (Turowski, Rickenmann, and Dadson, 2010). The total sediment available for the lower Mekong regions, therefore, can range from 54 to 76 million ton. This is almost in line with the estimation of Lu, Kummu, and Oeurng (2014), which is about 50 million ton y^{-1}.

Although only part of the above estimated total load of sediment is available for the mangrove forest, it still seems to be enough for the estuarine mangroves. To keep up with the subsidence rate of about 2 cm y^{-1} in the MES (Anthony *et al.*, 2015), the amount of sediment needed for the 16,000 ha of estuarine mangrove (100 m width, 200 km length, eight branches) is estimated at only around 8.5 million tons (about 10% of the total, available sediment load). In fact, that amount is probably smaller because the width of mangrove tends to reduce upstream, and some branches merge around 30–100 km. Hence, the deficiency of sediment sources is not considered a primary reason for the degradation of the estuarine mangrove forest. This study, therefore, focused on the degradation of the estuarine mangrove due to the "squeeze" issue, *i.e.* a limited mangrove width because of the extension of fish farms.

The term *squeeze* was introduced by Doody (2004) in recognition of the threat to the existence of coastal mangroves or tidal wetland habitats caused by the compound impacts of sea-level rise and human activities. The term has been widely used since (Gilman, Ellison, and Coleman, 2007; Torio and Chmura, 2013). Gilman, Ellison, and Coleman (2007) noted that, when relative sea level is rising, mangrove forests tend to retreat landward. However, the spatial blocking induced by

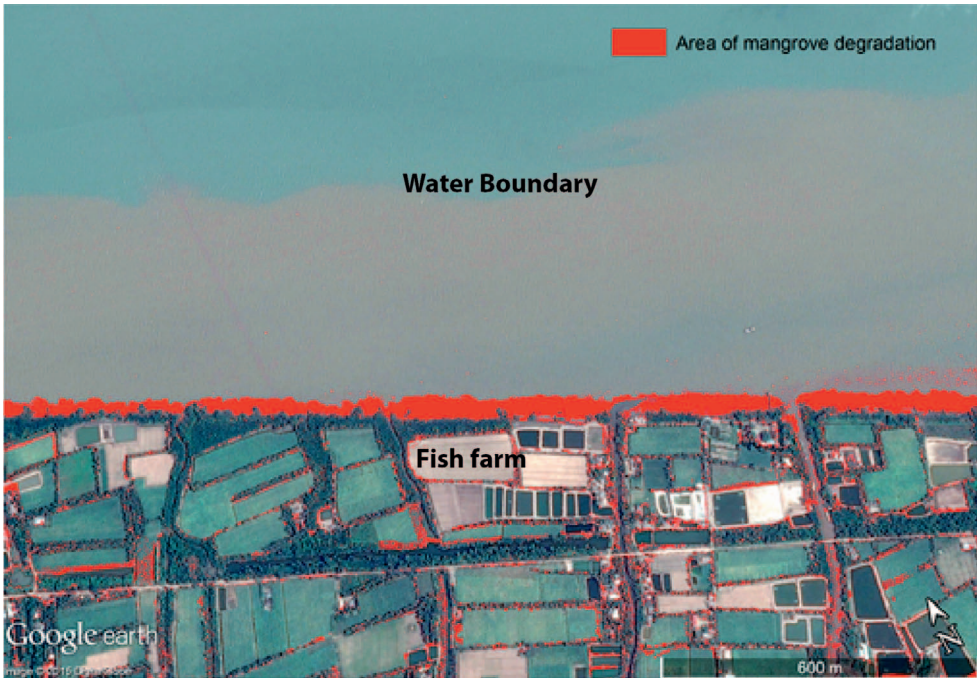

Figure 2. Mangrove degradation along a straight part of Dinh An Estuary in An Thanh province (location 14). The red area illustrates the loss in mangrove area from 2006 to 2014. Fish farms constructed close to the water boundary pushed the mangrove into a narrow fringe zone. This area is suffering from erosion at a rate of about 2.5 m y^{-1}.

human activities, such as urbanization, agriculture, and aquaculture, prevents the ecosystem from retreating, pushing the mangroves into narrower and narrower fringes and, finally, to disappear entirely (Feagin *et al.*, 2010). A certain space, therefore, is needed for the ecosystem to be able to retreat to when sea-level rise affects the coast. Phan, van Thiel de Vries, and Stive (2014) adopted the term *squeeze* to determine a "minimum width" required for coastal mangroves to be able to develop sustainably. Nevertheless, in the MES, the situation is even more serious. Mangroves have regularly been cleared for conversion into aquaculture. Fish farms have been constructed intensively, extending toward the foreshore, and pushing mangroves to narrow strips. This squeeze phenomenon is a threat to the existence of the mangroves, even when the availability of sediment is not an issue. Although sea-level rise is a threat from the water boundary, the destruction of mangroves for conversion to aquaculture is a threat from the land boundary. The latter usually happens in a shorter period and with a larger order of magnitude than the former. Natural sand-dune coasts, salt-marsh coasts, and mangrove coasts are ecosystems that form a transition between the open water and the land. There are both abiotic and biotic arguments suggesting that a certain minimal width is required by these ecosystems, and that remains true for fringing estuarine mangroves, as well. Space is required for energetic conditions to be absorbed, and vegetation needs to be able to follow a cyclic evolution. This means that a "minimum width" is required for the survival of the ecosystem, whether the impacts come from relative sea-level rise or from human activities.

METHODS

The study area and the mangrove forests in their local and international context are described, followed by an analysis of the observations of estuarine mangrove widths and estuarine bank morphology. Next, to increase understanding about the hydrodynamic forcing in a mangrove forest, a numerical model was applied to study the penetration of flow from the main river channel into the mangrove forest. It was hypothesized that a link existed between estuarine mangrove squeeze and the maximum distance in which flow penetration occurs. This hypothesis has not been considered in the international literature.

Study Site in Global and Regional Contexts

Based on the continental borders, mangroves can be found in six tropical regions: western America, eastern America, western Africa, eastern Africa, Indo-Malaysia, and Australia (Duke, 1992). Mangroves in Vietnam belong to the Indo-Malaysian class, the class with the greatest biodiversity (Alongi, 2002). Lugo and Snedaker (1974), based on a functional classification of mangrove forests, categorized mangrove into six classes, namely, fringing, riverine, overwash, basin, scrub, and hammock mangroves. Cintron and Novelli (1984), studying topographic landforms, simplified that classification into three main classes: fringing, riverine, and basin mangroves. Woodroffe (1992), studying the important role of two physical processes in mangrove forests, namely, the unidirectional river flows and the bidirectional tidal flows, proposed a general classification by referring to mangrove

habitats as occupying a broad continuum between tide-dominated mangroves, river-dominated mangroves, and those mangrove forests that are isolated from either of those processes, as interior mangrove. Ewel, Twilley, and Ong (1998) proposed a hybrid of these systems, combining the classification system of Lugo and Snedaker (1974) with the general system of Woodroffe (1992). Their simplified classification system refers to tide-dominated mangroves as *fringe mangroves*, river-dominated mangroves as *riverine mangroves*, and interior mangrove as *basin mangroves*. Riverine mangroves or river-dominated mangroves are flooded by river water as well as by tides. They usually dominate in the river-dominated deltas and are mostly exposed to unidirectional water flows during flood tides. Fringing or tide-dominated mangroves usually dominate low-gradient, intertidal areas of a sheltered coastline. They are usually inundated by daily tides and exposed to strong bidirectional tidal flow. Fringing mangroves facing the open sea (coastal mangrove) can also be exposed to waves. Interior mangroves usually dominate in inland depressions, where they are least exposed to waves and tidal motions (Ewel, Twilley, and Ong, 1998; Lugo and Snedaker, 1974; Woodroffe, 1992).

All the above state-of-the-art classification systems consider only tides and river flows as the major hydrodynamic indicators, and wave actions were not considered. Although the role of mangroves in dissipating wave energy and protecting coastal regions has been well recognized, little attention has been given to the reverse effects of waves on mangroves. Waves have a role in the resuspension of bottom sediments (Wolanski, 1994). There is also a difference in the impact of short waves and long waves on mangroves (Phan, van Thiel de Vries, and Stive, 2014).

Neglecting the wave factor makes it more difficult to understand the differences in the setting of coastal mangroves and estuarine mangroves, which is particularly true for the MES. The Mekong Delta is classified as both a wave-influenced and a tide-dominated delta, according to the ternary diagram of Galloway (1975) (Ta, Nguyen, and Tateishi, 2002). The tide in the region has a semidiurnal character. The mean tidal range is 2.6 m (Gagliano and McIntire, 1968), whereas the maximum tidal range is 3.2–3.8 m (Nguyen, Ta, and Tateishi, 2000; Wolanski *et al.*, 1996). The average depth of the estuarine branches is typically 5–10 m in the regions between the river mouth and up to 140 km upstream (Wolanski *et al.*, 1996). Because of the relative low elevation and gentle slope of the delta, tides and salt water can intrude deeply into the floodplain through the estuaries of the Mekong and the Bassac River (Tri, 2012). In the dry season, tidal variation can be observed as far as Tan Chau and Chau Doc, 228 km upstream from the river mouth (Wolanski *et al.*, 1996). Because of these specific features, mangrove forests in the Mekong Delta dominate a wide range of areas from the coastal to estuary and further upstream. Those differences in the regions where mangroves dominate implies differences in the hydrodynamic forces affecting mangrove populations (Figure 3). Although coastal mangroves are distributed alongshore and are often exposed to waves, estuarine mangroves are much less exposed to sea waves and storms. Estuarine mangroves usually dominate in floodplains, which have gently sloping substrates (2–3%) that are exposed at low tides and flooded at high tides. They can also be flooded by river water. Salinity varies during the different flood and dry seasons. Therefore, the mangrove setting is different from that found in coastal to estuarine areas. This was confirmed in the observations of Phan and Hoang (1993). In the coastal area, dense forests are usually found, with trees 15–25 m tall, composed *Rhizophora*, *Sonneratia*, and *Avicennia* species. Coastal mangrove forest width is usually >100 m, with a complex tidal creek systems. In estuarine areas, *Sonneratia* community species dominate, along with a mixed community of *Avicennia alba*, *Nypa fruticans*, and *Derris trifoliata*. Further inland, along the river, mostly *Avicennia* species and *Nypa fruticans* develop with *Derris trifoliata*. The mangrove forest width along the river is usually <50 m.

The simplification of state-of-art classification systems can be challenged. Based on observations of the mangrove forest in the Mekong Delta, a new classification is proposed, with three main categories: fringing coastal mangroves (FCs), fringing estuarine mangroves (FEs), and the interior mangrove (I). FCs are the mangrove forests dominating coastal regions and are primarily exposed to waves and tide. FEs are the mangrove forests dominating in estuarine regions, primarily controlled by tidal forces and the geometric features of the river. The influence of tidal flow, river flow, and lateral flow are important for FE mangrove forests. Those mangroves that are protected and least exposed to the forces of waves and tides can be classified as I mangroves. In this study, only the FE mangroves were analyzed.

The mangrove area in the Mekong Delta, Vietnam, accounts for about 70% of the entire mangrove habitat in Vietnam, about 109,000 ha in 2005 (Food and Agriculture Organization, 2007). Recently, many changes have been observed in the mangrove forests of the Mekong Delta. During the Vietnam War (1962–71), nearly 40% of the mangrove forests in the region were destroyed (Phan and Hoang, 1993). Mangrove forests started to recover around 1975 because of natural generation and manual planting. In the 1980s and early 1990s, the mangrove forests were heavily affected by timber overexploitation and the conversion of forest land into aquaculture–fishery farming systems (Christensen, Tarp, and Hjortso, 2008). Forest felling bans were imposed by the mid-1990s, but then ceased in 1999. Since then, many mangrove forests have been cleared to create areas for shrimp farming. Currently, many of the eight estuaries of the Mekong Delta are degraded, and the destruction of mangrove forests have been observed. In those regions, only narrow strips of about 10–50 m of mangrove forest remain in front of fish farms.

The literature has focused considerably more attention on the loss of coastal mangroves. The effects of wave action are usually blamed as the important cause of mangrove degradation. Anthony and Gratiot (2012), based on an analysis of the impact of land use on coastal mangroves in Guyana, found that the loss of mangroves reduced wave dissipation and promoted net erosion within the mangrove area. According to Winterwerp *et al.* (2013), there are two main reasons for the unsuccessful rehabilitation of coastal mangrove systems: the reduction in the onshore, fine-sediment flux because of a decrease in onshore water flux, and local scour in front of

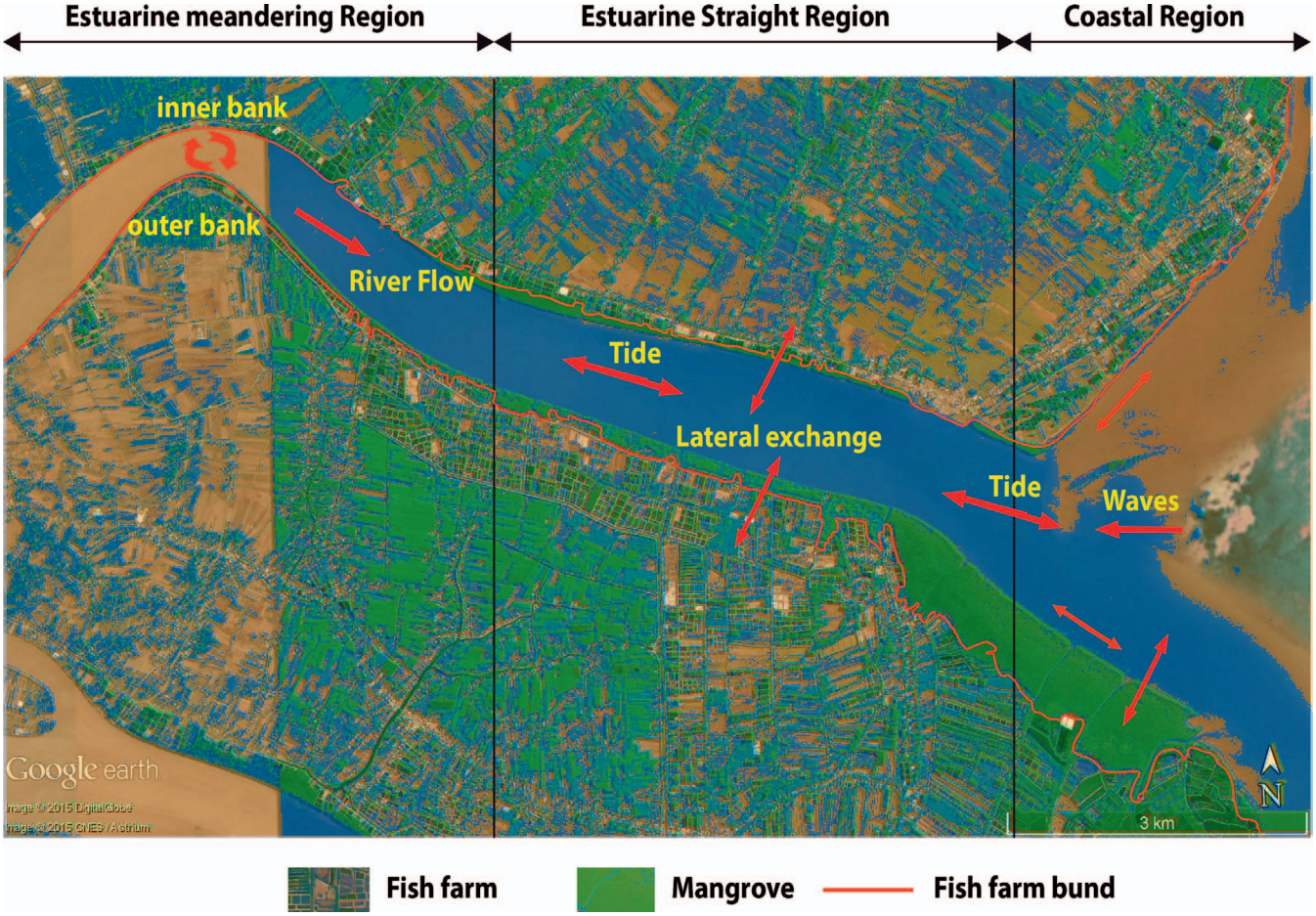

Figure 3. Mangroves at Tieu Estuary. The hydrodynamic forces differ between the river and the sea environment. Coastal mangroves are often exposed to sea waves and storms. Estuarine mangroves are much less exposed to those elements. Instead, estuarine mangroves are influenced by lateral flow and the geometric features of the river (meandering or straight).

structures because of a local increase in wave height due to reflection caused by the implementation of structures within the mangrove forests. In observations of the coastal area of the Mekong Delta, Phan, van Thiel de Vries, and Stive (2014) proposed a relationship between coastal evolution and mangrove width and suggested the important role of long-wave penetration in the sustainability of mangroves.

However, as mentioned, coastal mangroves and estuarine mangroves have different hydrodynamic forces. Whereas coastal mangroves are controlled by wave attenuation, estuarine mangroves are controlled by lateral flow, at least on the bank close to the river. The effects of waves are small in estuarine mangroves. Furthermore, in estuarine regions, several other hydrodynamic factors can lead to the erosion of riverbanks, such as meandering effects and circulation flow. Therefore, the squeeze relationship between mangrove forest width and evolution rate developed for coastal areas cannot readily be applied to mangroves in estuarine regions.

This study focused on the straight part of the estuaries to eliminate the meandering effect. The fundamental hypothesis was that there must be a critical minimum width for an estuarine mangrove forest fringe to exist sustainably exist or, once surpassing the minimum width, to favor sedimentation. The flow penetration into the mangrove forest needs a certain distance to reach an equilibrium-damping value. If the width of the forest is larger than that distance, there will be enough space to absorb the parallel flow energy and to promote sediment deposition, offering a successful environment for both propagules and sedimentation. If the width of the forest is smaller than that distance, the flow energy inside the forest will not have decreased to a reasonable level. Seeds and propagules cannot survive, and sediment cannot be accumulated. A mangrove forest in such a state will degrade, and the riverbank will suffer from more erosion.

Observations of Mangrove Width and Riverbank Evolution

The estuarine squeeze hypothesis, *i.e.* whenever fish farms or dikes are constructed too close to the nonvegetated foreshore, suggests that erosion trends will dominate and,

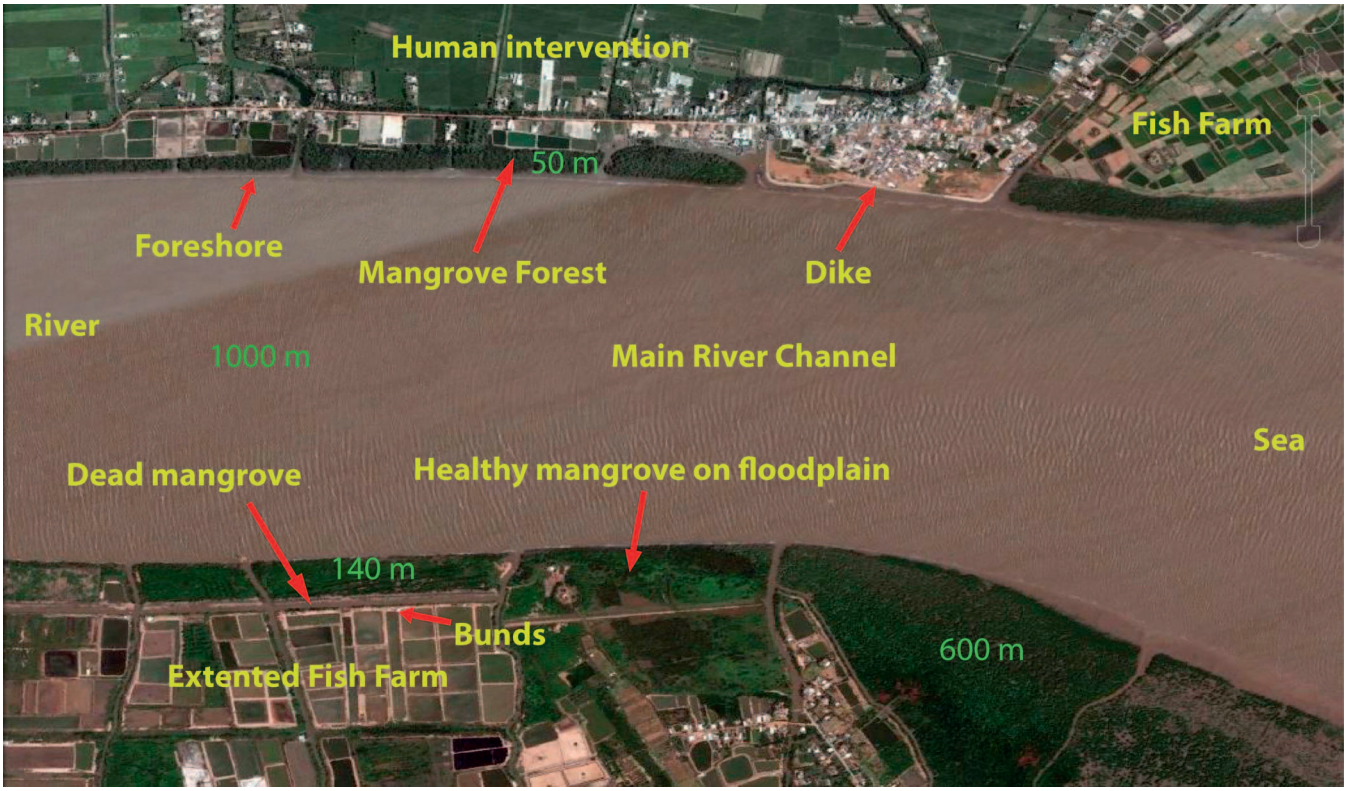

Figure 4. Google Earth image of mangrove distribution along the Tieu Estuary in the MES. In this 5-km stretch of an almost-straight estuary, the mangrove forest has been strongly disturbed by local fish farms and dikes. The tidal creeks cannot be seen.

consequently, the health of the mangrove forest will be threatened.

Optical satellite observations confirm that human intervention, especially the construction of fish farms, has disturbed mangrove forests in all branches of the MES. Figure 4 shows a part of Tieu Estuary with its existing mangrove forest, reflecting a typical situation for the estuarine mangroves in the MES. The fish ponds were extended toward the foreshore. Few mangroves can be observed in front of hard structures, such as dikes. The remaining width of a mangrove forest depends principally on the extent of the fish farms.

In the MES, fish farms have expanded continuously toward the foreshore (Figure 5). In Figure 5, the green line represents the landward boundary in 2006, and the orange line represents the landward boundary in 2010. Between 2006 and 2010, the fish farms extended, with a resulting degradation of the mangrove forest.

In the estuarine regions, at meandering locations, sedimentation can occur on the inner bank of the river, whereas on the outer bank, erosion occurs, and mangroves collapse if their foundations are eroded. Thus, the meandering locations are more complex, where both natural and human-induced impacts occur. That will be a topic for further study. In this study, to eliminate the meandering effect, observations are focused only on the straight parts of the estuaries. Eight estuaries were reviewed; of which, three were disregarded. In Ba Lai Estuary, the construction of the Ba Lai dam created morphology changes that are different from other branches of the MES, and the resolution of satellite images captured for the Co Chien and Cung Hau estuaries were too low to be used to

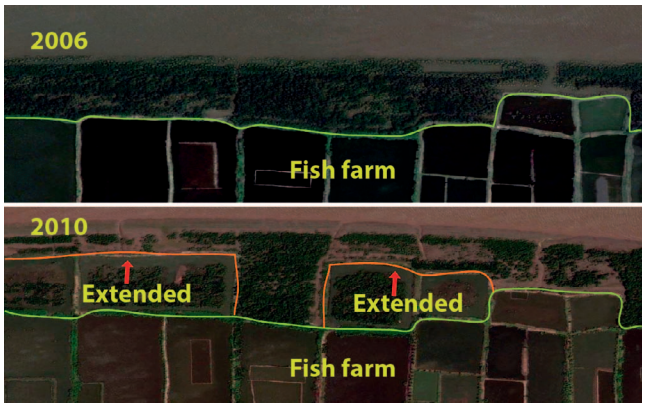

Figure 5. Google Earth image showing a typical example of the change in mangrove forests between 2006 and 2010 at the Dai Estuary from extended fish farms. Converted mangrove areas are blocked area, resulting in the redistribution of sediments, which causes the area of unhealthy mangroves to increase.

Table 1. *Average riverbank evolution rates reported in 2006 (SIWRR, 2010) and Google-Earth–based, estimated mangrove widths in 2006 in the MES at different branches.*

No.	Location	Length (km)	Situation	Riverbank Evolution Rate (m y^{-1})	Mangrove Width Range (m)	Representative Mangrove Width (m)
1	Middle of Tan Hoa–End of Tan Hoa	3	Accretion	1.5	35–60	50
2	Phu Dong	7	Stable	0	100–190	140
3	Phu Tan	5	Accretion	4.5	550–700	600
4	Middle of Phu Thanh to Phu Dong	—	Accretion	2.5	110–290	250
5	Middle of Phu Dong	3	Erosion	−1.5	20–110	85
6	Dinh Trung–Binh Thoi	5	Erosion	−2.5	0–40	25
7	Binh Thoi commune	—	Erosion	−1.5	0–30	20
8	Binh Thang commune	2.5	Accretion	1	45–75	50
9	An Hiep to An Duc	—	Erosion	−2.5	0–60	50
10	An Duc–An Hoa Tay	—	Stable	0	30–170	90
11	An Thanh	4	Accretion	1	50–120	85
12	An Dien	5	Accretion	4	350–600	500
13	Tra Cu Province–Ham Giang	8	Erosion	−3.5	0–75	40
14	An Thanh 2- An Thanh 3	8	Erosion	−2.5	20–120	55
15	Dai An 1	7	Erosion	−1.5	10–60	35
16	Co Tron River -Sea	2.5	Stable	0	50–90	75
17	Dai An 2	—	Erosion	−1.5	20–70	30

measure mangrove width. Tieu, Dai, Ham Luong, Dinh An, and Tran De branches offered the most favorable observations, with clear and high-resolution images available. At selected locations, the mangrove width could be measured, the fish ponds could be clearly identified, and data on evolutionary rate were available.

The following assumptions are applied to the observations. Firstly, the area of interest was the area from the landward boundary of the fish ponds to the nonvegetated foreshore. It was assumed that the mangrove width of that area was a representative mangrove width for the entire cross section. Secondly, the mangroves, because of conditions necessary for their survival, usually develop as entire forests, not as individual plants; therefore, the mangrove observations focused on the entire mangrove forest.

An investigation report from the Southern Institute of Water Resources Research (SIWRR, 2010) indicated locations suffering from erosion and accretion. For this study, the mangroves width observed in those areas are represented with minimum widths, maximum widths (mangroves width range), and representative mangroves widths. The observations were taken at different locations that had experienced either erosion or sedimentation on the Tieu, Dai, Ham Luong, Dinh An, and Tran De branches (chosen locations are numbered 1–17 in Figure 1; location names can be found in Table 1). According to scale classifications of shores and shoreline variability presented by Stive *et al.,* 2002, this study was interested in evolutionary trends based on a timescale of years to decades, with a space scale of 1–10 km. Mangrove widths for each location observed were measured from Google Earth for the year 2006 and are presented in Table 1. The rate of riverbank evolution in 2006 is presented in Table 1.

The suggested relationship between mangrove width and estuarine-bank evolution is shown in Figure 6, which presents the average evolutionary rate as a function of mangrove width in 2006. The uncertainty bars were applied in both vertical and horizontal directions. The uncertainty in the width variability was not due to ground-referencing errors (the location of the primary dike was not influenced by water levels, for instance), but rather, the uncertainty was the result of alongshore variability over the stretches considered and included in the data presentation. The vertical bars indicate the estimated uncertainty in the evolutionary rate given by SIWRR (2010), which, on average, was 0.5 m y^{-1}. A power trend line was fitted that included the 90% confidence interval. Although interpretation of results can be somewhat subjective, from Figure 6, it can be deduced that the riverbank will remain stable in the presence of a mangroves width range of approximately 50–150 m, with a representative value of about 80 m. A larger width would lead to a healthier fringe and higher sedimentation potentials. The data set was limited to those locations in which sediment availability was not expected to be a constraint. In general, riverbank evolution depends on many factors, such as local sediment supply, local hydraulic conditions (flow, wave, wind, current), local bathymetry, *etc*. Hence, no unique critical mangrove-width value can be set for all estuarine regions. The quantitative relationship provided, therefore, is only applicable

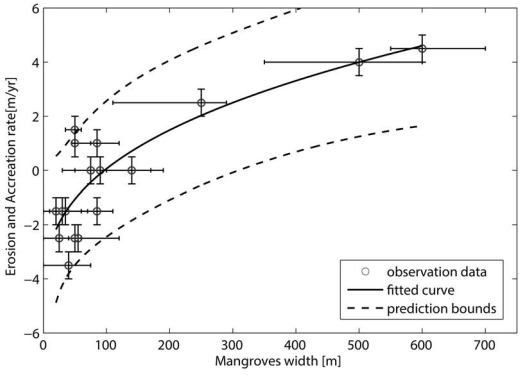

Figure 6. The relationship between mangrove forest width and riverbank evolution in the Mekong Delta Estuaries (assuming sediment availability is no constraint; see text).

to the Mekong and Bassac estuaries of the Mekong Delta, although the general principle will apply to many other estuarine mangrove regions.

Flow Attenuation in the Mangrove Forest

To study how far the flow from the river's main channel penetrated into the mangrove forest, and even more specific, the effectiveness of mangroves to attenuate flow energy as a function of mangrove width, were assessed. A state-of-the-art Delft3D-Flow model with a rigid vegetation simulation was applied. A schematized geometry based on the dimension of the Tieu estuary was used.

Hydrodynamics of Estuarine Mangrove Forest

As mentioned, although the primary hydrodynamic impacts on mangroves in a coastal area are waves, mangroves in estuaries are primarily affected by flow, *i.e*. flow caused by tidal action and by river discharge. Previous studies of the hydrodynamics of mangrove, in general, and in the Mekong Delta Estuaries, in particular, were based on particular field settings. Those studies investigated flow routing *i.e*. the flow in and out of a mangrove swamp. Flooding of the mangrove forest was discovered to have caused by a combination of over-bank flow and creek flow, and ebbing occurred primarily through creek flow (Aucan and Ridd, 2000). The distinction of creek-flow stage and over-bank flow stage was confirmed by comparing the results of a numerical model with data collected from field observations (Horstman, 2014). Flow routing was directly related to hydrodynamic routing of waterborne particles, such as mangrove seeds, nutrients, and fine, suspended sediments through the mangrove systems, which is thought to have an important role in supplying sediment and nutrients to mangroves (Furukawa, Wolanski, and Mueller, 1997; Mazda, Kanazawa, and Wolanski, 1995; Wolanski, Jones, and Bunt, 1980; Wolanski *et al.*, 1990). The significant friction induced by mangroves causes the deceleration of the tidal currents and a delayed discharge into the mangrove forest, resulting in a net input of sediments into the mangrove forest (Wattayakorn, Wolanski, and Bjerfve, 1990). This is known as the *tidal asymmetry* of tidal currents in both the tidal creeks and mangrove swamps.

That research was implemented principally within healthy riverine mangrove forests, in which mangrove width was not limited and was much larger than the region of the lateral over-bank flow. However, in the MES, only a narrow strip of mangrove forest is left because of the human impacts. The mangrove width observed in the MES (approximately 50–600 m) is small when compared with the main estuarine channel width of 1000–2000 m. Few transversal tidal creeks were observed in the study area. The flow routing in a mangrove forest without tidal creeks is different from that in forests with tidal creeks. By collecting the flow-velocity data along a cross section through a smoothly sloping riverine mangrove fringe without creeks, flow velocities were observed to be parallel to the river at the forest fringe but gradually turned perpendicular to the river further into the forest (Kobashi and Mazda, 2005). That finding accentuates the important role of lateral exchanges in a mangrove forest without creeks. In this sense, the mangrove forests in the MES are similar to vegetated floodplains, which have been explored by several researchers, primarily in laboratory setting. These studies of vegetated floodplains, including a one-dimensional model (Helmio, 2004; Ikeda, Izumi, and Ito, 1991; Vionnet, Tassi, and Wide, 2004) and a two-dimensional model (Pasche and Rouve, 1985), focused on the momentum-exchange mechanism, the distribution of the total discharge, and the distribution of the averaged flow velocity between the main channel and the vegetated floodplain.

In the literature, the similarity in flow hydrodynamics between mangroves and vegetated floodplains has been recognized (Mazda *et al.*, 1997). The shear-layer vortices caused by the Kelvin-Helmholtz instability formed at the interface of the vegetated regions has a significant role in the lateral momentum exchange (well recognized by Nadaoka and Yagi, 1998; Nezu and Onitsuka, 2000; Tamai, Asaeda, and Ikeda 1986; van Prooijen, Battjes and Uijttewaal, 2005; White and Nepf, 2007, 2008; Xiaohui and Li, 2002; Zong and Nepf, 2010). Nevertheless, those realizations have not been integrated into studies of the hydrodynamics of mangroves. White and Nepf (2007) proposed a model for the vortex-included exchange and the penetration of momentum into a vegetated floodplain. However, that model was based on only one set of flume experiments with rigid, circular cylinders, so whether that result was valid generically has yet to be determined (Nepf, 2012). The exchange of mangrove seeds, nutrients, and fine, suspended sediments through this mechanism can be fundamental for a sustainable mangrove forest.

In summary, because of an estuarine squeeze, the mangrove width in the MES is usually very narrow. In this situation, the hydrodynamics of the mangrove forest is similar to that of a vegetated floodplain. Lateral tidal creeks can be disregarded. The main interaction is the lateral-momentum exchange through the shear-layer vortices between the main river channel and the floodplain region with the mangroves. This momentum exchange is considered to have an important role in the sustainable development of the mangrove forest. The maximum penetration length into the mangrove forest of that momentum exchange during periods of high river discharge were estimated through a depth-averaged velocity profile predicted by a schematized model constructed in Delft3D-FLOW.

Estuarine Mangrove Distribution

To construct the schematized model for the mangroves in the MES, it was necessary to increase the detail on the mangrove types available within these estuarine regions. Mangroves grow mainly between mean sea level and highest spring tide (Alongi, 2009; Hogarth, 1999) because, below mean sea level, the mangrove seedlings cannot settle, and above the highest spring tide levels, the mangroves cannot compete with the other plants (Schiereck and Booij, 1995). The succession form of the mangrove forest system in the MES, including the mangrove species that dominate land edges and those that dominate water edges, can be described as experiencing the following main stages (Phan and Hoang, 1993). The Pioneer Stage is usually found on tidal flats flooded by the mean tide. Mangrove species, such as *Sonneratia* and *Avicennia*, are able to tolerate the extensive flooding and high salinity. They have the same biological characteristics of pneumatophores roots,

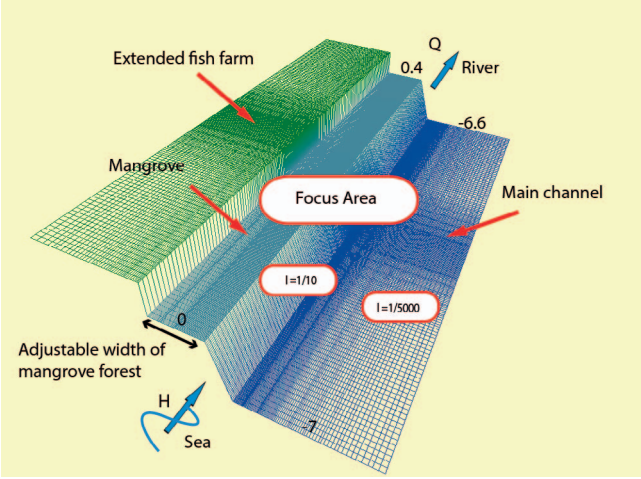

Figure 7. A 3D schematized model of the Tieu Estuary. The model includes a main river channel and a floodplain. It covers the first 2-km stretch from the river mouth and half of the estuarine width.

which can rapidly establish themselves in the substrate. The Transition Stage is a stage in which the pneumatophore system of *Sonneratia* and *Avicennia* species trap and hold soil and alluvium. After a short time, the mudflats are elevated, *i.e.* when sediment is available as a source. Seedlings of other land-edge species, such as *Nypa fruticans*, *Cryptocoryne ciliata*, and *Acanthus ilicifolius* are carried to the flats by tidal water and trapped by the pneumatophore system. The final stage is a Multispecies Community. Because the land is continuously elevated by alluvial deposition, it is usually only flooded at high tide and more land-edge mangrove species, such as *Derris trifoliate*, *Wedelia biflora*, and *Acanthus*, *ilicifolius* are able to develop.

In contrast to coastal mangroves, estuarine mangroves consist of a variety of mixed types that are able to adapt to a wide range of salinities, such as *Sonneratia Alba*, *Avicennia alba*, and *Acanthus ilicifolius*, *Nypa fruticans*, *Cryptocoryne ciliata*, *etc*. In the Mekong Delta Estuaries, the presence of Rhizophora is not often observed, except in the Ba Lai Estuary (Phan and Hoang, 1993). In the schematized model, the estuarine mangrove forest was considered to consist only of *Sonneratia* species. This type of mangrove is known by its pneumatophores, which are erect, lateral branches of horizontal cable roots that grow underground (De Vos, 2004).

Schematized Model, Different Scenarios, and Input Parameters

To obtain insight into the efficiency of a mangrove forest in reducing the impact of alongshore flow, as well as the penetration scale of the shear layer into the forest, a schematized model of mangroves in the Tieu Estuary was constructed in Delft3D. The model covered the first 2 km from the river mouth and half of the estuarine width (1100 m). Default settings in Delft 3D were used as much as possible. Specific settings are explained below and are related to bathymetry, hydraulic boundary conditions, vegetation properties, and numerical choices.

The bathymetry and the hydrodynamics were schematized to provide input into the Delft3D-FLOW vegetation model. The model includes a main river and a floodplain in the form of a trapezium-shaped channel. The bathymetry and the slope of the estuary were estimated using topographic maps from the SIWRR (2010) report. Because of the gentle slope of the substrate in a mangrove forest, a mangrove forest slope was not attempted but was taken as being horizontal. (Figure 7)

Hydraulic boundary conditions of the model consisted of river discharge upstream and water level downstream. Because the study area was located in a region of tidal influences, an upstream boundary condition was needed for the model. This was created by extending the model 200 km upstream to the Vam Nao channel, where the tide influence is negligible during the flood season. A constant discharge value could be applied to that location. The water level downstream was recorded by an acoustic Doppler current profiler on 15–30 September 2009. In this extended model, the discharge at 2 km from the river mouth was extracted and applied as the upstream boundary condition for the smaller, nested model. Subsequently, the nested model with a constant boundary condition was set up by considering only a representative time during which the depth-averaged velocity in the main river channel was largest because the largest penetration of the flow into the mangrove forest was expected to occur when the depth-averaged velocity in the main river reached its maximum value and was accompanied by the greatest difference between the depth-averaged velocity in the main channel and that in the mangrove forest. A representative moment in time was chosen at 0500 on 20 September 2009 (Figure 8), when the water level recorded at the river mouth equaled 0.48 m, and the discharge value was 2848 $m^3 s^{-1}$.

As mentioned, only one type of mangrove—*Sonneratia* sp.—was considered. The characteristics of the *Sonneratia* sp. are described with nine parameters and three different layers by Narayan *et al*. (2011) for the mangroves in India. The similarities between the mangrove species in the Mekong Delta and those in India were the argument for using those parameters in the current model (Table 2).

Several mangrove widths, from 50 m to 300 m, were considered. For each case, three scenarios of mangrove density (spare density, average density, and dense density) were examined. The basic setup with the scenarios is presented in Table 3.

To estimate the penetration-length scale of the shear-layer vortices into the mangrove forest, the results focused on the depth-averaged velocity in the middle cross section of the model (the high-resolution area in Figure 7), where a fully developed region with stable flow conditions of uniform velocity across the mangrove forest and the main river channel existed.

RESULTS

The impacts of extending fish farms toward the nonvegetated foreshore were studied by reducing the mangrove width toward the floodplain edge (at $x = 600$ m). The depth-averaged velocity distribution and its reduction trend across the estuary from the main channel to the mangrove forest were examined for no, spare, average, and dense vegetation scenarios. The overall

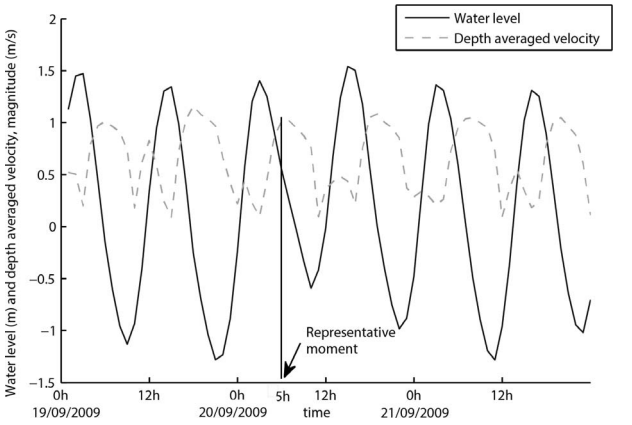

Figure 8. Water level and velocity at the Tieu Estuary and a representative moment in time chosen for a constant boundary condition.

model results are presented in Figure 9, showing the reduction trend of the depth-averaged flow velocity from the main channel to inside the mangrove forest. The depth-averaged velocity profiles in the case without mangroves are presented in Figure 10. The reduction level in the depth-averaged velocity for different vegetation densities is shown in Figure 11. Figure 12 focuses on the overall deceleration of the depth-averaged velocity in the region around the last 200 m of the floodplain area (from 450 m to 650 m).

General Results

In general, the model results indicated that the depth-averaged velocity in the main channel with mangroves was faster than it was without mangroves, and the depth-averaged velocity in a floodplain area with mangroves was much slower than it was without mangroves (Figure 9). In other words, the velocity gradient between the main channel and the floodplain increased with the presence of vegetation. This corresponds with the presence of vegetation in the floodplain inducing drag forces, thus reducing the overall flow velocity.

In the case with mangroves, the depth-averaged velocity in the main channel was on the order of magnitude of 0.9 m s^{-1}, which quickly reduced to an order of magnitude of 0.015 m s^{-1} inside the mangrove forest ($u_{channel}/u_{mangrove} = 35$), in line with that measured in previous studies (Anthony, 2004; Horstman, 2014; Van Santen *et al.,* 2007). The velocity gradient between the main channel if the river and mangrove forest was about four times larger than that between the adjacent tidal creeks (0.1 m s^{-1}) and the mangrove swamp ($u_{creeks}/u_{mangrove} = 10$). This difference in the velocity gradient again emphasizes the important role of the lateral exchange between the main river channel and the mangrove swamp.

Table 2. *Vegetation parameters (adapted from Narayan* et al., 2011).

Parameters	*S. Alba*		
Stem diameter (m)	0.3		
Root diameter (m)	0.02		
Canopy diameter (m)	0.5		
Stem height (m)	6		
Root height (m)	0.5		
Canopy height (m)	2		
Density Variations	Spare	Average	Dense
Stem density (m^{-2})	0.5	0.7	1.7
Root density (m^{-2})	25	50	100
Canopy density (m^{-2})	50	100	100

Table 3. *Different scenarios for the Tieu Estuary in the schematized model in Delft 3D-Flow*.

Schematized Model	Floodplain Width (m)	Mangrove Width (m)	Q (m^3 s^{-1})	H (m)
Tieu Estuary	300	300	2848	0.48
	200	200	2848	0.48
$i = 1/5000$	50	50	2848	0.48
$i_f = 1/10$	300, 200, 50	No mangroves	2848	0.48
$L = 2$ km, $B = 1.15$ km				

Q = river discharge upstream, H = water level downstream, i = slope of river bed, i_f = slope of river bank, L = length of river section, B = width of river.

No Mangroves

In the cases without mangrove forests, the magnitude of the velocity within the floodplain region varied with the changes in the floodplain width (Figure 10). The smaller the floodplain was, the larger the depth-averaged flow velocity within the floodplain area was. The depth-averaged velocity at the beginning of the floodplain ($x = 600$ m) was about 0.35 m s^{-1}. In the cases of 300-m and 200-m floodplain widths, the depth-averaged velocity reduced and achieved a uniform value of about 0.15 m s^{-1} (43% of that at the start of the floodplain water edge) after about 150 m. With a 50-m floodplain width, the depth-averaged velocity reduced to about 0.3 m s^{-1} (86%) after 50 m. This implies that the depth-averaged flow velocity needs a certain distance from the floodplain edge to achieve a uniform value.

Mangrove Forests with Different Densities

The uniform depth-averaged flow velocity within the mangrove forest of Tieu Estuary model was, as anticipated, to reach around 0.015 m s^{-1}, and that value reduced slightly when the density of the mangroves increased (Figure 11). Figure 11 also shows that, together with the increasing vegetation density, the depth-averaged velocity profiles around the edge of the mangrove forest was steeper and required a shorter distance ($x = 600$ m) to achieve uniform values within the mangrove forest. This result implies that if the mangrove forest width is not restricted, the penetration of the exchange into the vegetation regions caused by the velocity gradient between the main channel and the vegetated area is principally dependent on the vegetation characteristics.

Mangrove Forests with Different Widths

The trend toward reduced distance from the main channel to the inside of the mangrove forest by the depth-averaged flow velocity was quite similar in cases of 300-m mangrove widths, 200-m mangrove widths, or 50-m mangrove widths for the Tieu Estuary (Figure 9). By looking in more detail into the region around the last 150 m of mangrove edge (from $x =$ 450 m to $x = 600$ m) (Figure 12), the model indicated that the depth-averaged velocity required about 60–80 m to reach a

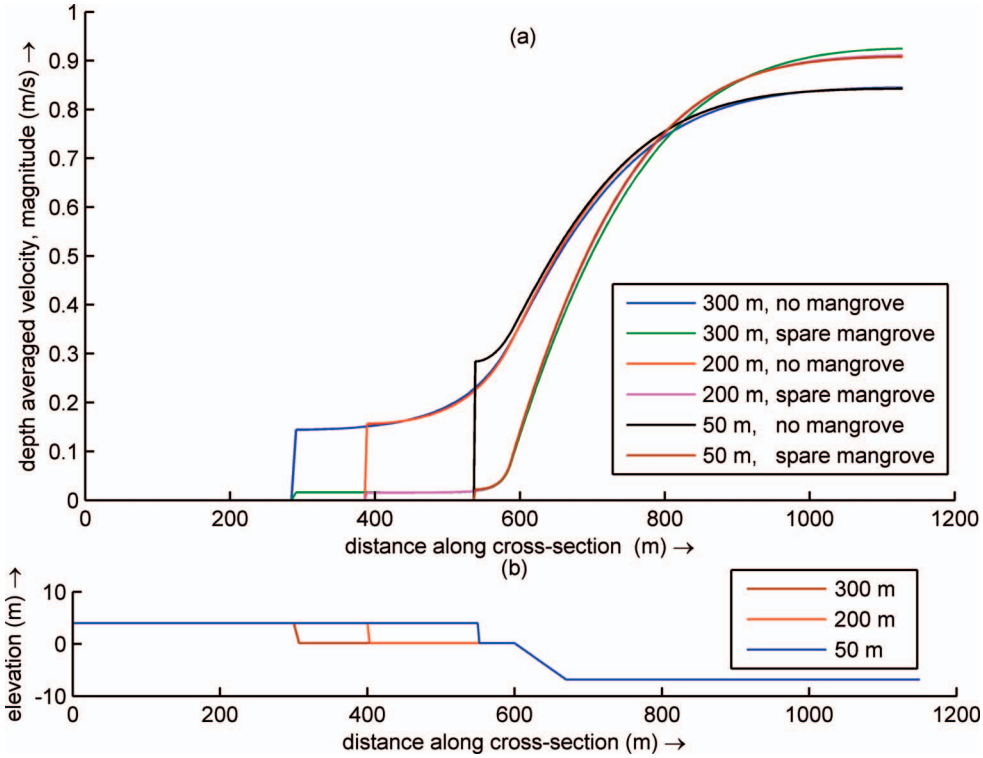

Figure 9. Depth-averaged velocity along the cross section of the Tieu Estuary schematized model (a) and the corresponding profile with 300-m, 200-m, and 50-m floodplain widths (b) (from the equilibrium profiles).

fully uniform value within the mangrove forest (about 0.015 m s^{-1}). That depth-averaged velocity was about 20% of that at the start of the forest (0.08 m s^{-1}). This implies that the length scale of the penetrating shear layer into the mangrove forest was 60–80 m. In other words, the minimum distance from the mangrove edge at which the velocity in the mangrove forest reached a uniform value of about 0.015 m s^{-1} was about 60–80 m. Therefore, when floodplain widths were less than 60–80 m, the depth-averaged velocity profile in the mangrove forest would not reach a uniform value because the penetration length of the mixing layer was larger than the width of the mangrove forest.

In conclusion, these results show that, as long as the riverine mangrove forest width in the MES is larger than approximately 60–80 m, the uniform depth-averaged flow velocity within the mangrove forest is dependent on mangrove characteristics, rather than on the characteristics of bathymetry and hydraulic conditions in the adjacent main river channel. However, when the riverine mangrove forest width is less than 60–80 m, the uniform depth-averaged velocity within the mangrove forest is affected by the flow in the main river channel. This is in agreement with the observations that confirm the hypothesis of the existence of a link between critical mangrove width in the estuarine mangrove forest and the maximum penetration of the flow into the forest. An averaged value of 80 m is the minimum width at which the mangrove forest can be maintained, and at that width the forest is sustainable if the construction of fish farms does not reduce that width.

DISCUSSION

The physical meaning of a critical mangrove width can be discussed within the context of sedimentation and forest-restoration capacity.

Critical Mangrove Width and Sedimentation

The requirements for a sustainable mangrove forest are very strict. Significant changes in the sediment dynamics within a mangrove forest can do damage to the entire system. Too much sedimentation may bury the mangrove propagules, leading to the death of the aerial mangrove root system of the pioneer species, such as *Sonneratia* and *Avicenna*. However, too little sedimentation may lead to the destabilization of the mangrove trees. The mangrove propagules have a length of 25–30 cm, so a sediment thickness of around 30 cm is necessary to provide a suitable environment for mangrove aerial roots (Phan, 2012). Nevertheless, only 10 cm of root burial can make *Avicennia* trees die (Ellison, 1998), and 8 cm of sediment burial can reduce growth and increase mortality of *Rhizophora* seedlings (Terrados *et al.*, 1997). In addition, because mangrove roots anchor in only about 0.5 m of the soil, a few decimeters of erosion is sufficient to destabilize a mangrove tree (Winterwerp *et al.*, 2013).

Once fish ponds are constructed too far into the mangrove forest, insufficient mangrove width remains for a proper lateral

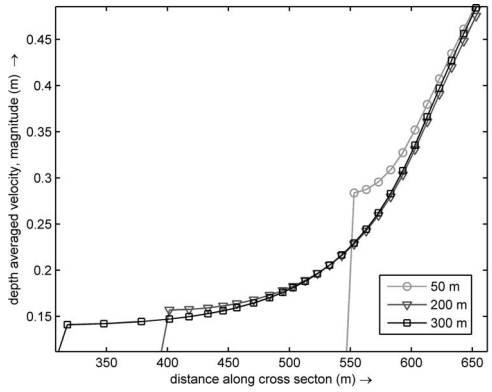

Figure 10. Depth-averaged velocity along the cross section of the Tieu Estuary schematized model for floodplains of 50, 200, and 300 m widths without mangroves.

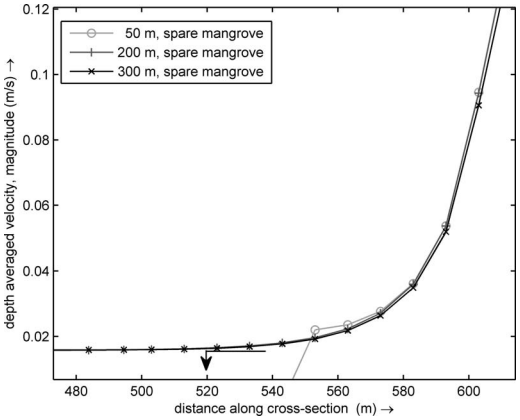

Figure 12. Depth-averaged velocity in the floodplain region of the Tieu estuarine model.

exchange between the main river channel and the adjacent mangrove forest; this critical width is estimated to be, on average, about 80 m. Widths less than that directly disturb the hydrodynamic conditions, leading to changes in sediment source as well as the available space for sedimentation, reducing the total capacity of the mangrove forest to trap sediment. If there is no accommodation space available, sediment will bypass those sites and be transported to an area in which accommodation space allows the sediment to be deposited (Coe, 2003). Similarly, sediment that cannot be deposited in converted mangrove areas will be transported and deposited in adjacent area, where it may bury mangrove propagules. Therefore, the readjustment of the sedimentation system will have a negative impact on the adaptive capacity of the mangrove system. The loss of mangroves will again reduce the sediment-trapping capacity, resulting in more erosion of the riverbank.

Critical Mangrove Width and Restoration Capability

Mangrove forests affected by human intervention landward can sometimes be restored, but only by monocultures of fast-growing species, such as *Sonneratia*, *Avicenna*, or *Rhizophora*;

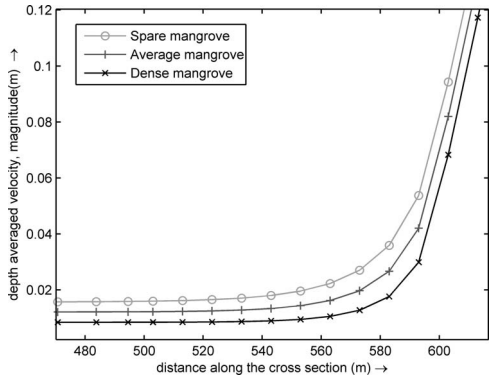

Figure 11. Depth-averaged velocity showing different vegetation-density scenarios at the Tieu Estuary. The result is focused on the floodplain region.

rarer species and entire mangrove ecosystems cannot be fully restored. This phenomenon of unsuccessful restoration of mangrove ecosystems, especially that of rare land-edge species, was recently reported by Polidoro *et al*. (2010).

The reasons for this phenomenon may be explained by the hypothesis about the connection between critical mangrove width and the width of the earlier-stage mangrove species. As mentioned, the primary threats to mangroves are landward human interventions and waterborne sea-level rise. Although human interventions directly affect the mangrove species at the land edges—those established in the final successional stage, the effects of sea-level rise threatens the mangrove species at the water edges—those established in the pioneer stage. However, those mangrove species establishing in the later stages are more vulnerable to sea-level rise than are mangrove species that are established at earlier stages because the later-stage mangroves grow slower, have greater difficulty with dispersal, and reproduce slower than do the mangrove species at earlier stages, such as *Sonneratia* and *Avicennia* species (Polidoro *et al*., 2010). Mangrove species at the water edges of a mangrove forest can be considered a "pioneer protection layer" for land-edge mangrove forests because they cope better with changes at the open-water side, such as sea-level rise, than do the inner mangrove species. Any changes in the open water side first affect the protection layer, and the inner layer has more time to respond to those changes (such as landward retreat). That protection is necessary to the sustainability of the entire mangrove forest ecosystem. The rules for the transition from pioneer species to the species associated with transitional and climax stages are unknown. It was, therefore, hypothesized that there is a link between the critical minimum width and the width of the protection layer for the later stages of mangrove species. In other words, the critical minimum width is also the width that the pioneer mangrove species need for the succession of in the forest to further stages. Once, the human intervention on the land side block mangrove forest reaches and exceeds that width, all the later-stage mangrove species are destroyed (if they already exist) or they do not have space to develop (if they do not already exist)

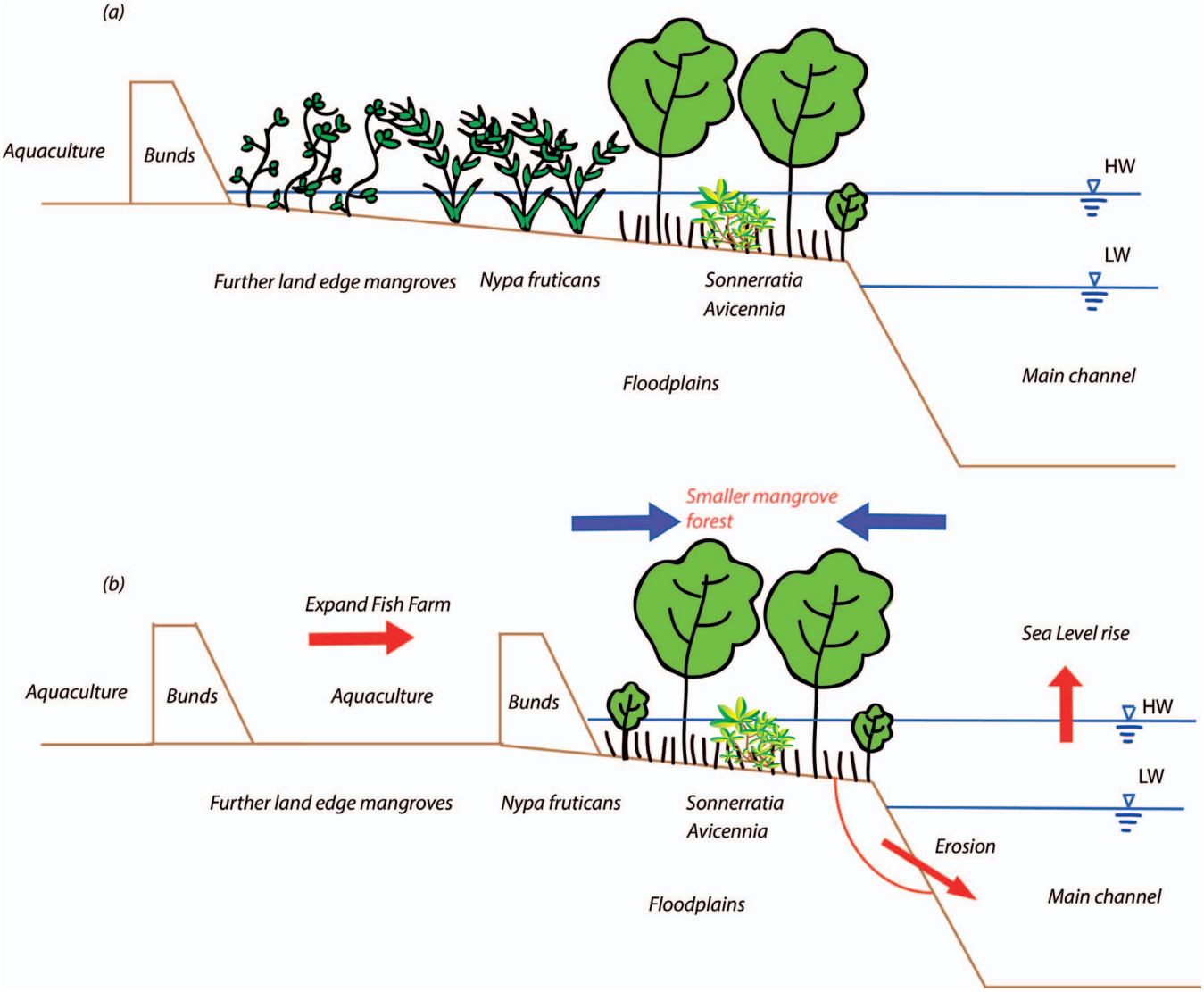

Figure 13. The impact of different levels of fish farm expansion on successive stages of the mangrove forest in the MES (following Phan and Hoang, 1990) (a) and the estuarine mangrove squeeze issues in Mekong Delta Estuaries (b).

(Figure 13), preventing the mangrove forest from reaching its successive stages.

Flow kinetic energy is proportional to the velocity squared. Therefore, the forces absorbed (F_{absorb}) per meter of mangrove forest width can be modeled as followed:

$$F_{\text{absorb}} \sim \frac{K_{\text{no-mangrove}} - K_{\text{mangrove}}}{Width} \quad \text{or}$$
$$F_{\text{absorb}} \sim \frac{U^2_{\text{no-mangrove}} - U^2_{\text{mangrove}}}{Width} \qquad (1)$$

The forces absorbed per meter of mangrove forest width for various different widths are estimated in Figure 14. According to that estimation, when reducing from 200–300 m to 50–55 m of mangrove width, the magnitude of the forces absorbed per meter of width increases on an order of 10. That means that, for every meter of width, a 50-m mangrove forest absorbs forces that are about 10 times greater than those absorbed by every meter of 200-m or 300-m forests to reduce the average velocity to a value suitable for the development of mangroves. Therefore, when a mangrove forest is reduced from 300 m to 50 m, the force per unit meter that the mangrove forest needs to absorb increases about 10 times. Under those new conditions, only the pioneer mangrove species can survive and develop. However, many fish farms and other human interventions have been constructed within forests in which the mangrove species are in their final successional stages, which means they are weaker, more vulnerable, and will likely die.

These results mean that if, for some reason, the entire 50 m or 300 m of estuarine mangroves were to be destroyed and the propagules of mangrove species were replanted in those

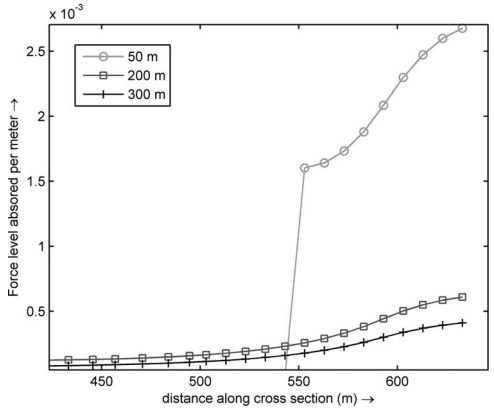

Figure 14. Force level the mangrove forest is required to absorb per meter of width with different mangrove forest widths shown (Tieu Estuary model).

regions, the force the forest would need to absorb would be 10 times greater for the 50-m forest. This implies that the larger the width of a mangrove forest, the easier it is for that forest to recover, especially for the land-edge mangrove species.

CONCLUSIONS

In this study, mangrove forest degradation and the trends in riverbank evolution affected by the extent of fish farms in the MES were analyzed by adopting a broader definition of the term *estuarine squeeze*. In that context, a minimum width was derived that the estuarine mangrove ecosystem needs for healthy, cyclic evolution. If mangrove forest widths are less than 80 m in the MES, the riverbank will be less stable and the estuarine mangroves will be more vulnerable. The results were estimated based on an empirical relationship between mangrove forest width and riverbank evolution. Based on the similarity between the hydrodynamics of a narrow mangrove forest and that of a vegetated floodplain channel, the exchange mechanism between the main river channel and the vegetated floodplain could be identified. That mechanism controls such fundamental factors as the transport and deposition of sediment, the supply of nutrients, and the significance of organic outwelling from a mangrove forest. This occurs because of the penetration of shear-layer vortices caused by the velocity gradient and the presence of mangroves on the floodplain. Results from the Delft3D-flow vegetation model for the Tieu Estuary showed the penetration length scale of the shear layer into the mangrove forest. The depth-averaged flow velocity from the main channel was reduced to a uniform value on an order of magnitude of 0.015 m s^{-1} within 60–80 m inside the mangrove forest. The agreement between field observations and the schematized model confirmed the existence of and estuarine mangrove squeeze and the hypothesis of a critical width linked to the maximum penetration of the flow into the mangrove forest.

Unsuccessful mangrove restoration attempts at the land edge of the forest, which usually contains more rare and vulnerable species compared with pioneerspecies, can be explained by assuming a link between the critical minimum width and the minimum width of the mangroves at a pioneer stage. The difficulty in the recovering mangrove species in their final stages (the land edge of the mangrove forest) can also be understood from an energetic standpoint.

Future work will concentrate on further validation of the model results by both field work and laboratory experiments in terms of both hydrodynamics and sedimentation.

ACKNOWLEDGMENTS

This study was supported by the Ministry of Education and a training scholarship (MOET), Vietnam; the Technical University Delft, The Netherlands; The Water Resources University of Hanoi, Vietnam; and the Southern Institute of Water Resources Research of Vietnam.

LITERATURE CITED

Alongi, D.M., 2002. Present state and future of the world's mangrove forest. *Environmental Conservation,* 29(3), 331–349.

Alongi, D.M., 2008. Mangrove forests: Resilience, protection from tsunamis, and responses to global climate change. *Estuarine, Coastal and Shelf Science*, 76, 1–13.

Alongi, D.M., 2009. *The Energetics of Mangrove Forests*. Queensland, Australia: Springer, 216p.

Anthony, E.J., 2004. Sediment dynamics and morphological stability of estuarine mangrove swamps in Sherbro Bay, West Africa. *Marine Geology,* 208(2–4), 207–224.

Anthony, E.J.; Brunier, G.; Besset, M.; Goichot, M.; Dussouillez, P., and Nguyen, V.L., 2015. Linking rapid erosion of the Mekong River Delta to human activities. *Science Report*, 5, 14745. doi: 10.1038/srep14745

Anthony, E.J. and Gratiot, N., 2012. Coastal engineering and large-scale mangrove destruction in Guyana, South America: Averting an environmental catastrophe in the making. *Ecological Engineering,* 47, 268–273.

Aucan, J. and Ridd, P.V., 2000. Tidal asymmetry in creeks surrounded by saltflats and mangrove with small swamp slopes. *Wetlands Ecology and Management,* 8(4), 223–232

Baptist, M.J., 2005. Modelling Floodplain Biogeomorphology. Delft, The Netherlands: Delft University Technology, Ph.D. dissertation, 274p.

Bouma, T.J.; Van Duren, L.A.; Temmerman, S.; Claverie, T.; Blanco-Garcia, A., and Ysebaert., 2007. Tidal flow and sedimentation patterns within patches of epibenthic structures: Combining field, flume and modelling experiments. *Continental Shelf Research,* 27(8), 1020–1045.

Christensen, S.M.; Tarp, P., and Hjorts, C.N., 2008. Mangrove forest management planning in coastal buffer and conservation zones, Vietnam: A multi methodological approach incorporating multiple stakeholders. *Ocean and Coastal Management,* 51(10), 712–726.

Cintron, G. and Schaeffer-Novelli, Y.S., 1984. Methods for studying mangrove structure. *In*: Snedaker, S.C. (ed.), *The Mangrove Ecosystem: Research Methods*. Paris: UNESCO, pp. 91–113.

Coe, A.L. (ed.), 2003. *The Sedimentary Record of Sea-Level Change*. Cambridge, U.K.: Cambridge University Press, 294p. http://catdir.loc.gov/catdir/toc/cam041/2004296450.html.

De Vos, W.J., 2004. Wave Attenuation in Mangrove Wetlands: Red River Delta, Vietnam. Delft, The Netherlands: Delft University of Technology, Master's thesis, 107p. http://repository.tudelft.nl/view/ir/uuid%3A4d8f93b5-8efa-4663-a29a-448a50c45525/.

Deltares, 2014. *Delft3D-FLOW User Manual: 3D/2D Modelling Suite for Integral Water Solutions—Hydro-Morphodynamics*. Deltares, Delft: Deltares Systems, 684p.

Doody, J.P., 2004. 'Coastal squeeze'—An historical perspective. *Journal of Coastal Conservation,* 10(1), 129–138.

Duke, N.C., 1992. Mangrove floristics and biogeography. *In*: Robertson, A.I. and Alongi, D.M. (eds.), *Tropical Mangrove Ecosystems*. Washington D.C.: American Geophysical Union, pp. 63–100.

DWW (Hydraulic Engineering Department), 2004. *Bank Erosion in Mekong Delta and along Red River in Vietnam: Report Mission 23 November–6 December 2003*. Delft, The Netherlands: Road and Hydraulic Engineering Division, Rijkswaterstaat, 172p.

Ellison, J.C., 1998. Impacts of sediment burial on mangroves. *Marine Pollution Bulletin,* 37(8–12), 420–426.

Ewel, K.C.; Twilley, R.R., and Ong, J.E., 1998. Different kinds of mangrove forest provide different good and services. *Global Ecology and Biogeography Letters,* 7(1), 83–94.

FAO (Food and Agriculture Organization), 2007. *The World's Mangroves 1980–2005*. Rome: FAO, *Forestry Paper 153*, 77p.

Feagin, R.A.; Martinez, M.L.; Mendoza-Gonzalez, G., and Costanza, R., 2010. Salt marsh zonal migration and ecosystem service change in response to global sea level rise: A case study from an urban region. *Ecology and Society,* 15(4), 1–14.

Furukawa, K.; Wolanski, E., and Mueller, H., 1997. Current and sediment transport in mangrove forests. *Estuarine, Coastal and Shelf Science,* 44(3), 301–310.

Gagliano, S.M. and McIntire, W.G., 1968. *Reports on the Mekong River Delta*. Baton Rouge, LA: Coastal Studies Institute, *Louisiana State University Technical Report 57*, 144p.

Galloway, W.E., 1975. Process framework for describing the morphologic and stratigraphic evolution of deltaic depositional systems. *In*: Broussard, M.L. (ed.), *Deltas: Models for Exploration*. Houston: Houston Geological Society, pp. 87–98.

Gebhardt, S.; Lam, D.N., and Kuenzer, C., 2012. Mangrove ecosystems in the Mekong Delta—Overcoming uncertainties in inventory mapping using satellite remote sensing data. *In*: Renaud, F.G. and Kuenzer, C. (eds.), *The Mekong Delta System: Interdisciplinary Analyses of a River Delta*. Heidelberg, Germany: Springer, pp. 315–330.

Gilman, E.; Ellison, J., and Coleman, R., 2007. Assessment of mangrove response to projected relative sea-level rise and recent historical reconstruction of shoreline position. *Environmental Monitoring and Assessment,* 124(1–3), 105–130.

Helmio, T., 2004. Flow resistance due to lateral momentum transfer in partially vegetated rivers, *Water Resources Research,* 40(5), 1–10.

Hogarth, P.J., 1999. *The Biology of Mangroves*. Oxford: Oxford University Press, 228p.

Horstman, E.M., 2014. The Mangrove Tangle: Short-Term Bio-Physical Interactions in Coastal Mangroves. Twente, The Netherlands: University of Twente, Ph.D. dissertation, 141p.

Hu, K.; Ding, P.; Wang, Z., and Yang, S., 2009. A 2D/3D hydrodynamic and sediment transport model for the Yangtze Estuary, China. *Journal of Marine Systems,* 77(1–2), 114–136.

Ikeda, S.; Izumi, N., and Ito, R., 1991. Effects of pile dikes on flow retardation and sediment transport. *Journal of Hydraulic Engineering,* 117(11), 1459–1478.

International Union for Conservation of Nature, 2011. *Why Healthy Ecosystems Matter: The Case of Mangroves in the Mekong Delta*. http://iucn.org/about/union/secretariat/offices/asia/regional_activities/building_coastal_resilience/?8865/Why-healthy-ecosystems-matter-the-case-of-mangroves-in-the-Mekong-delta.

Kobashi, D. and Mazda, Y., 2005. Tidal flow in riverine-type mangrove. *Wetlands Ecology and Management,* 13(6), 615–619.

Kummu, M. and Varis, O., 2007. Sediment-related impacts due to upstream reservoir trapping, the Lower Mekong River. *Geomorphology,* 85(3–4), 275–293.

Lu, X.X.; Kummu, M., and Oeurng, C., 2014. Reappraisal of sediment dynamics in the Lower Mekong River, Cambodia. *Earth Surface Processes and Landform,* 39(14), 1855–1865.

Lu, X.X. and Siew, R.Y., 2006. Water discharge and sediment flux changes over the past decades in the Lower Mekong River: Possible impact of the Chinese dams. *Hydrology and Earth System Sciences,* 10(2), 181–195.

Lugo, A.E. and Snedaker, S.C., 1974. The ecology of mangroves. *Annual Review of Ecology and Systematics,* 5(1), 39–64.

Manh, N.V.; Dung, N.V.; Hung, N.N.; Merz, B., and Apel, H., 2014. Large-scale suspended sediment transport and sediment deposition in the Mekong Delta. *Hydrology and Earth System Science,* 18, 3033–3053.

Mazda, Y.; Kanazawa, N., and Wolanski, E., 1995. Tidal asymmetry in mangrove creeks. *Hydrobiologia,* 295(1), 51–58.

Mazda, Y.; Wokanski, E.; King, B.; Sase, A.; Ohtsuka, D., and Magi, M., 1997. Drag force due to vegetation on mangrove swamps. *Mangrove and Salt Marshes,* 1(3), 193–199.

Milliman, J.D. and Farnsworth, K.L., 2011. *River Discharge to the Coastal Ocean: A Global Synthesis*. New York: Cambridge University Press, 384p.

Milliman, J.D. and Ren, M.E., 1995. River flux to the sea: Impact of human intervention on river systems and adjacent coastal areas. *In*: Eisma, D. (ed.), *Climate Change: Impact on Coastal Habitation*. Boca Raton, Florida: Lewis, pp. 57–83.

Nadaoka, K. and Yagi, H., 1998. Shallow-water turbulence modeling and horizontal large-eddy computation of river flow. *Journal of Coastal Engineering,* 124(5), 493–500.

Narayan, S.; Suzuki, T.; Stive, M.J.; Verhagen, H.; Ursem, W.; and Ranasinghe, R., 2011. On the effectiveness of mangrove in attenuating cyclone-induced waves. *Proceedings of the International Conference on Coastal Engineering*, 32: 1–12.

Nepf, H.M., 2012. Hydrodynamics of vegetated channels. *Journal of Hydraulic Research,* 50(3), 262–279.

Nezu, I. and Onitsuka, K., 2000. Turbulent structures in partly vegetated open-channel flows with lda and piv measurements. *Journal of Hydraulic Research,* 39(6), 629–642.

Nguyen, V.L.; Ta, T.K.O., and Tateishi, M., 2000. Late Holocene depositional environments and coastal evolution of the Mekong River Delta, Southern Vietnam. *Journal of Asian Earth Science,* 18(4), 427–439.

Pasche, E. and Rouve, G., 1985. Overbank flow with vegetative roughened floodplains. *Journal of Coastal Engineering,* 111(9), 1262–1278.

Phan, K.L., 2012. The Mekong Deltaic Coast: Past, Present and Future Morphology. Delft, The Netherlands: Delft University of Technology, Master's thesis, 121p.

Phan, K.L.; van Thiel de Vries, J.S.M., and Stive, M.J.F., 2014. Coastal mangrove squeeze in the Mekong Delta. *Journal of Coastal Research,* 31(2), 233–243.

Phan, N.H. and Hoang, T.S., 1993. *Mangroves of Vietnam*. Bangkok: IUCN, 173p.

Polidoro, B.A.; Carpenter, K.E.; Collins, L.; Duke, N.C.; Ellison, A.M.; Farnsworth, E.J.; Fernando, E.S.; Kathiresan, K.; Koedam, N.E.; Livingstone, S.R.; Miyagi, T.; Moore, G.E.; Ngoc Nam, V.; Ong, J.E.; Primavera, J.H.; Salmo, S.G., III; Sanciangco, J.C.; Sukardjo, S.; Wang, Y., and Yong, J.W.H., 2010. The loss of species: Mangrove extinction risk and geographic areas of global concern. *PLoS One* 5(4), e10095. doi:10.1371/journal.pone.0010095

Schiereck, G.J. and Booij, N., 1995. Wave transmission in Mangrove Forest. *Proceedings of the International Conference in Coastal and Port Engineering in Developing Countries* (Rio de Janeiro, Brazil, PIANC), pp. 1969–1983.

SIWRR (Southern Institute of Water Resources Research), 2010. *Tien Estuary Investigation Report*. Ho Chi Minh, Vietnam: Ministry of

Agriculture and Rural Development of Vietnam, 180p (in Vietnamese).

Stive, M.J.F.; Aarninkhof, S.G.; Hamm, L.; Hanson, H.; Larson, M., and Wijnberg, K.M., 2002. Variability of shore and shoreline evolution. *Coastal Engineering,* 47(2), 211–235.

Ta, T.K.O.; Nguyen, V.L.; Tateishi, M.; Kobayashi, I.; Saito, Y., and Nakamura, T., 2002. Sediment facies and Late Holocene progradation of the Mekong River Delta in Ben Tre Province, southern Vietnam: An example of evolution from a tide-dominated to a tide- and wave-dominated delta. *Sedimentary Geology,* 152(3–4), 313–325.

Tamai, N.; Asaeda, T., and Ikeda, H., 1986. Study on generation of periodical large surface eddies in a composite channel flow. *Water Resources Research,* 22(7), 1129–1138.

Temmerman, S.; Bouma, T.J.; Govers, G.; Wang, Z.B.; De Vries, M.B., and Herman, P.M.J., 2005. Impact of vegetation on flow routing and sedimentation patterns: Three-dimensional modelling for a tidal marsh. *Journal of Geophysical Research,* 110(F4), 2156–2202.

Terrados, J.; Thampanya, U.; Srichai, N.; Kheowvongsri, P.; Geertz-Hansen, O.; Boromthanarath, S.; Panapitukkul, N., and Duarte, C.M., 1997. The effect of increased sediment accretion on the survival and growth of *Rhizophora apiculata* seedlings. *Estuarine, Coastal and Shelf Science,* 45(5), 697–701.

Torio, D.D. and Chmura, G.L., 2013. Assessing coastal squeeze of tidal wetlands. *Journal of Coastal Research,* 29(5), 1049–1061.

Tri, V.K., 2012. Hydrology and hydraulic infrastructure systems in the Mekong Delta, Vietnam. *In*: Renaud, F.G. and Kuenzer, C. (eds.), *The Mekong Delta System: Interdisciplinary Analyses of a River Delta*. Heidelberg, Germany: Springer, pp. 49–81.

Turowski, J.M.; Rickenmann, D., and Dadson, S., 2007. The partitioning of the total sediment load of a river into suspended load and bedload: A review of empirical data. *Sedimentology,* 57(4), 1126–1146.

Uittenbogaard, R.E., 2003. Modelling turbulence in vegetated aquatic flows. *Proceedings of the International Workshop on Riparian Forest Vegetated Channels: Hydraulic, Morphological and Ecological Aspects* (Trento, Italy). pp. 1–17.

van Leeuwen, B.; Augustijn, D.C.M.; van Wesenbeeck, B.K.; Hulscher, S.J.M.H., and de Vries, M.B., 2010. Modeling the influence of a young mussel bed on fine sediment dynamics on an intertidal flat in the Wadden Sea. *Ecological Engineering,* 36(2), 145–153.

van Prooijen, B.; Battjes, J., and Uijttewaal, W., 2005. Momentum exchange in straight uniform compound channel flow. *Journal of Hydraulic Engineering,* 131(3), 177–185.

Van Santen, P.; Augustinus, P.G.E.F.; Janssen-Stelder, B.M.; Quartel, S., and Tri, N.H., 2007. Sedimentation in an estuarine mangrove system. *Journal of Asian Earth Sciences,* 29(4), 566–575.

Vionnet, C.; Tassi, P., and Wide, J.M., 2004. Estimates of flow resistance and eddy viscosity coefficients for 2D modelling on vegetated flood-plains. *Hydrological Processes,* 18(15), 2907–2926.

Wattayakorn, G.; Wolanski, E., and Kjerfve, B., 1990. Mixing, trapping and outwelling in the Klong Ngao mangrove swamp, Thailand. *Estuarine, Coastal and Shelf Science,* 31(5), 667–688.

Webb, E.L.; Friess, D.A.; Krauss, K.W.; Cahoon, D.R.; Guntenspergen, G.R., and Phelps, J., 2013. A global standard for monitoring coastal wetland vulnerability to accelerated sea-level rise. *Nature Climate Change*, 3(5), 458–465.

White, B.L. and Nepf, H.M., 2007. Shear instability and coherent structures in shallow flow adjacent to a porous layer. *Journal of Fluid Mechanics,* 593, 1–32.

White, B.L. and Nepf, H.M., 2008. A vortex-based model of velocity and shear stress in a partially vegetated shallow channel. *Water Resources Research,* 44(1), W01412. doi:10.1029/2006WR005651

Winterwerp, J.C.; Erftemeijer, P.L.A.; Suryadiputra, N.; van Eijk, P., and Zhang, L., 2013. Defining eco-morphodynamic requirements for rehabilitating eroding mangrove–mud coasts. *Wetlands,* 33(3), 515–526.

Wolanski, E., 1994. *Physical Oceanography Processes of the Great Barrier Reef*. Boca Raton, Florida: CRC, 194p.

Wolanski, E.; Jones, M., and Bunt, J.S., 1980. Hydrodynamics of a tidal creek-mangrove swamp system. *Marine and Freshwater Research,* 31(4), 431–450.

Wolanski, E.; Mazda, Y.; King, B., and Gay, S., 1990. Dynamics, flushing and trapping in Hinchinbrook channel, a giant mangrove swamp, Australia. *Estuarine, Coastal and Shelf Science,* 31(5), 555–579.

Wolanski, E.; Nguyen, H.N.; Le, T.D.; Nguyen, H.N., and Nguyen, N.T., 1996. Fine-sediment dynamics in the Mekong River Estuary, Vietnam. *Estuarine, Coastal and Shelf Science,* 43(5), 565–582.

Woodroffe, C.D., 1992. Mangrove sediments and geomorphology. *In*: Robertson, A.I. and Alongi, D.M. (eds.), *Tropical Mangrove Ecosystems*. Washington, D.C.: American Geophysical Union, pp. 7–41.

Xiaohui, S. and Li, C.W., 2002. Large eddy simulation of free surface turbulent flow in partly vegetated open channels. *International Journal for Numerical Methods in Fluids,* 39(10), 919–937.

Zong, L. and Nepf, H., 2010. Flow and deposition in and around a finite patch of vegetation. *Geomorphology,* 116(3–4), 363–372.

APPENDIX

Delft3D-FLOW has been widely applied to simulate flow hydrodynamics in vegetated, shallow-water environments (Horstman, 2014; Hu *et al.*, 2009; Temmerman *et al.*, 2005; van Leeuwen *et al.*, 2010). The process-based Delft3D-FLOW model solves the three-dimensional (3D) or two-dimensional, depth-averaged, unsteady, shallow-water equations. The hydrodynamic model applies horizontal momentum equations, hydrostatic pressure relations, the continuity equation, the advection-diffusion equation, and a turbulence closure model (Deltares, 2014). To acquire more knowledge about the effects of vegetation on the shallow-water environment, a vegetation module has been developed in Delft3D. Initially developed as a one-dimensional, vertical, momentum equation with turbulence closures accounted for in the presence of the vegetation, (Baptist, 2005; Uittenbogaard, 2003) assumed a collection of rigid, vertical cylinders. This was implemented in Delft3D through the directional point model (DPM), which has been validated successfully (Uittenbogaard, 2003). Then, the implementation of DPM in three dimensions was calibrated and validated successfully for salt-marsh vegetation (Bouma *et al.*, 2007; Temmerman *et al.*, 2005) and mangrove forests (Horstman, 2014). In the 3D application of the DPM, a depth-independent, vegetation-induced friction force, $F(z)$ in N m^{-3}, determined from the flow drag around the vegetation elements, was added to the momentum equation:

$$F(z) = \frac{1}{2}\rho_w C_D n(z) D(z) |u(z)| u(z) \qquad (A.1)$$

where, ρ_w is the water density (in kg m^{-3}); C_D represents the cylindrical drag coefficient (–); $n(z)$ is the depth distribution of the number of cylindrical elements per unit area (in m^{-2}), with depth diameter $D(z)$ (m); and $u(z)$ is the horizontal velocity (in m s^{-1}) at elevation z (in m).

Momentum exchange is limited by the porosity of the vegetation, $1 - A_p(z)$, where $A_p(z)$ is the cross-sectional area of the vegetation, per unit area $A_p(z)$ (–):

$$A_p(z) = \frac{1}{4}\pi D^2(z) n(z) \quad (A.2)$$

The influence of the vegetation on vertical mixing is reflected by an extra source term T in the kinetic turbulent energy equation and an extra source term $T\tau^{-1}$ in the ε equation:

$$\frac{\partial k}{\partial t} = \frac{1}{1-A_p}\frac{\partial}{\partial z}\left[(1-A_p)\left(\upsilon + \frac{\upsilon_t}{\sigma_k}\right)\frac{\partial k}{\partial z}\right] + T + P_k - B_k - \varepsilon \quad (A.3)$$

$$\frac{\partial \varepsilon}{\partial t} = \frac{1}{1-A_p}\frac{\partial}{\partial z}\left[(1-A_p)\left(\upsilon + \frac{\upsilon_t}{\sigma_k}\right)\frac{\partial \varepsilon}{\partial z}\right] + T\tau^{-1} + P_\varepsilon - B_\varepsilon - \varepsilon_\varepsilon \quad (A.4)$$

where, k is the turbulent kinetic energy (in $m^2\ s^{-2}$); z denotes the vertical coordinate; σ is the scaled, vertical coordinate; ε is the dissipation in the transport equation for turbulent, kinetic energy (in $m^2\ s^{-3}$); υ is the fluid velocity (in $m\ s^{-1}$); t is time (in s); P_k is a production term in the transport equation for turbulent, kinetic energy (in $m^2\ s^{-3}$); B_k is a buoyancy flux term in the transport equation for turbulent, kinetic energy (in $m^2\ s^{-3}$); P_ε is a production term in the transport equation for the dissipation of turbulent, kinetic energy (in $m^2\ s^{-3}$); B_ε is a buoyancy term in the transport equation for the dissipation of turbulent, kinetic energy (in $m^2\ s^{-3}$); ε_ε is dissipation in the transport equation for the dissipation of turbulent, kinetic energy (in $m^2\ s^{-4}$); and $T(z)$ is the energy spent upon the fluid:

$$T(z) = F(z) \times u(z) \quad (A.5)$$

τ is the minimum of $\tau = \min(\tau_{free}, t_{veg})$ with the dissipation timescale of the free turbulence; τ_{free} is the dissipation timescale of the free turbulence; and t_{veg} is the dissipation timescale of eddies in between the plants of typical size, limited by the smallest distance in between the stems:

$$L(z) = C_l\sqrt{\frac{1-A_p}{n(z)}} \quad (A.6)$$

where, C_l is a coefficient reducing the scale of the geometrical length to the scale of the typical volume-averaged turbulence length. A coefficient of 0.8 was found to be applicable (Uittenbogaard, 2003).